

Received February 22, 2020, accepted March 7, 2020, date of publication March 18, 2020, date of current version March 30, 2020.

Digital Object Identifier 10.1109/ACCESS.2020.2981647

# UAV Cluster-Based Video Surveillance System Optimization in Heterogeneous Communication of Smart Cities

YONG JIN<sup>1</sup>, ZHENJIANG QIAN<sup>1</sup>, AND WEIYONG YANG<sup>2</sup>

<sup>1</sup>School of Computer Science and Engineering, Changshu Institute of Technology, Changshu 215500, China

<sup>2</sup>NARI Group Corporation (State Grid Electric Power Research Institute), Nanjing 211000, China

Corresponding author: Yong Jin (jinyong@cslg.edu.cn)

This work was supported in part by the Natural Science Foundation of the Jiangsu Higher Education Institutions of China under Grant 19KJB520020, in part by the Open Foundation of The Suzhou Smart City Research Institute, Suzhou University of Science and Technology, under Grant SZSCR2019019, in part by the Natural Science Foundation of Jiangsu Province in China under Grant BK20191475, in part by the Qing Lan Project of Jiangsu Province in China under Grant 2017 and Grant 2019, in part by the 333 High-Level Personnel Training Project of Jiangsu Province in China under Grant 2018, in part by the Key Areas Common Technology Tendering Project of Jiangsu Province in 2017 (Research on Information Security Common Technology of Industrial Control System), in part by the Science and Technology Project of State Grid Corporation in 2019 (Research on Lightweight Active Immune Technology for Power Monitoring System), “New Generation Information Technology” Industry-University-Research Innovation Fund Project of Ministry of Education in China under Grant 2018A01003, in part by the “Tiancheng Huizhi” Innovation and Education Fund Project of Ministry of Education in China under Grant 2018A03008, and in part by the “Zhirong Xingjiao” Industry-University-Research Innovation Fund Project of Ministry of Education in China under Grant 2018A01004.

**ABSTRACT** Video surveillance system is the integration of computers, networks, communications, and video CODEC, etc. Because of its distributed architecture, parallel image processing and ease of installation and expansion, it is widely used in many fields such as education, transportation and industry. However, there are some challenges of video surveillance applications in smart cities such as large scale of video events, low quality and big delay of video data transmission, and the loss of video surveillance data integrity. In order to solve the above problems, this paper designs a series of optimization algorithms and scheduling strategies based on Unmanned Aerial Vehicle (UAV) cluster. Firstly, we construct a full device coverage network with UAV cluster in heterogeneous communication environment of smart cities. Secondly, we formulate the scheduling problem of UAV cluster as bi-objective fragile bin packing problem, and design an optimal scheduling algorithm with constant approximation performance ratio. The simulation experimental results fully demonstrate the effectiveness, feasibility and robustness of the proposed solution in terms of system life cycle, video decodable frame rate, the ratio of UAV flight time to system life cycle, throughput and delay.

**INDEX TERMS** Smart city, video surveillance, unmanned aerial vehicle (UAV) cluster, scheduler, bin packing, heterogeneous communication.

## I. INTRODUCTION

Video surveillance system [1] includes front-end camera, transmission cable, video surveillance platform and its control system. Camera [2] is used to collect front-end video image signals, as well as video data transmission, control, display and calculation functions. Large-scale cameras are interconnected by wired or wireless networks to transmit and process video data. They are widely used in many fields, such

The associate editor coordinating the review of this manuscript and approving it for publication was Ying Li.

as safety production monitoring [3], automatic pipeline [4], automatic driving [5], and intelligent transportation [6], etc.

It is well known that *Smart City* is a strategic for effectively solving the problems of economic and social development, urban infrastructure [7], quality of resident life, environmental ecology [8]. Its evolution has entered a period of in-depth development, implementation and application, and technical support. The above issues have become the current research hot-spots. In order to meet the needs of comprehensive perception, extensive interconnection and intelligent processing of urban services [9] and monitoring [10], scenic spots, environmental pollution, sustainable video surveillance [11],

a large number of intelligent sensors and terminals of the Internet of Things (IoT) need to be deployed in and/or around the city. However, these video surveillance devices are generally deployed inside severe environment and depopulated zone such that they cannot provide stable and reliable sustainable data communication [12], [13] and video event processing.

To solve these problems, academia and industry have proposed a series of effective and sustainable solutions, such as energy sustainable IoT [14], emote microgrids [15], fog data centers [16], self-sustainable wireless sensor node [17], dense mobile crowd-sensing [18], sustainable data-link [19], [20], etc.

Specially, the assistant application of Unmanned Aerial Vehicle (UAV) is particularly prominent [21]–[25]. However, there are still a series of challenges: (1) how to schedule UAVs according to random video surveillance events; (2) how to improve the scheduling efficiency of UAV cluster and the efficiency of video data processing; (3) how to balance the flight efficiency of UAVs and the response efficiency of video events; (4) how to schedule the UAVs, wireless base stations and video surveillance devices. Our motivation is to design a robust, efficient and effective video surveillance system for smart cities. Therefore, we proposed a UAV cluster-based video surveillance optimization scheme for heterogeneous communication in smart cities, which can provide reliable, real-time and feasible services for large scale video surveillance application in smart city. The proposed solution not only can prolong the system life cycle but also enhance the video heterogeneous communication performance of the surveillance network. Specially, it can also improve the throughput, video quality and delay of the video surveillance system.

The main contribution of our research are as follows: (1) we construct a full device coverage network with UAV cluster; (2) we define the sustainable video surveillance guarantee problem as bi-objective minimum bin packing problem; (3) we design a constant approximation algorithm to address the above problem.

The rest of the paper is organized as follows. In Section II, we give the related work. Section III describes the UAV-cluster assisted video surveillance network. In Section IV, we present the heterogeneous communications schemes for UAV-cluster following the fragile bin packing problem. Section V presents the simulation results, and concluding remarks are given in Section VI.

## II. RELATED WORK

In this section, we will introduce some key issues and researches of video surveillance, smart city and UAV schedule.

First, A dynamic partial-parallel data layout was proposed in [26] for green video surveillance storage. It adopts partial-parallel strategy, which dynamically allocates the storage space with appropriate degree of partial parallelism according to performance requirement. Reference [27] presented

a new video sensor for multi-measurements in an aircraft cargo compartment. Reference [28] presented a novel intelligent processing and utilization solution for big surveillance video data transmission based on the event detection and alarming messages from front-end smart cameras. Reference [29] introduced a new deep multi-channel residual networks-based metric learning method for video surveillance by considering the metric learning problem in moving human localization. In [30], a unique approach was presented to utilize the existing video surveillance infrastructure and optimize electricity consumption in large indoor spaces.

Second, [31] provided an overview of the theoretical problems of video surveillance application, and some feasible approaches. Reference [32] proposed an approach for traffic monitoring that does not rely on probe vehicles, and do not require vehicle localization through GPS. An architecture for smart health monitoring system was proposed and implemented by creating a basic test-bed [33]. The authors of [34] proposed a novel video visual analytical system for interactive exploration of surveillance video data, which consists of providing analysts with various views of information related to moving objects in a video.

Third, [35] investigated how to simultaneously ensure the reliability of the remote-control signal for multiple UAVs. Reference [36] proposed a methodology with a heuristic based on earliest available time algorithm which assigns tasks to UAVs with an objective of minimizing the make span. The UAV enabled secure communication system proposed in [37] can maximize the worst-case secrecy rate among the users within each period by jointly adjusting UAV trajectories and the users scheduling under the maximum UAV speed constraints, the UAV return constraints, etc. Reference [38] proposed a multi-objective path planning framework to explore a suitable path for a UAV operating in a dynamic urban environment.

## III. UAV CLUSTER ASSISTED VIDEO SURVEILLANCE SYSTEM

In the urban area, large-scale video surveillance devices are deployed randomly. Here, there is a difficulty, *i.e.*, using wired power supply and replacing batteries for them. Then, a series of wireless Base Stations (**BS**) would be deployed in the region to collect the data from the above devices. And these **BS**s form a rectangular boundary, as shown in Figure 1. The coverage area of each **BS** is represented by a *disk* model. Thus, it is the coverage area of the **BS** that the intersection of the circular rectangular area of the outer boundary and the rectangular red border of the inner boundary in Figure 1. If the video surveillance device is deployed in this area, it can establish direct connection with the **BS**. The triangle represents a video surveillance device that cannot be covered<sup>1</sup> by a **BS**. We connect several **BS**s to all video surveillance devices by deploying some UAVs. The black circle in Figure 1

<sup>1</sup>A device can be covered by a **BS** when their distance is smaller than the communication distance of the **BS**.

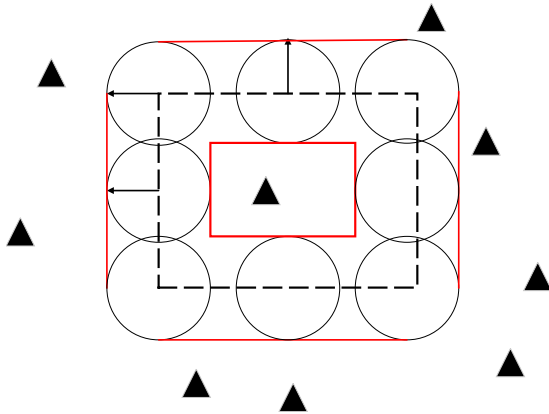


FIGURE 1. Coverage and reachable area of BS.

shows the coverage disk of the BS as the center and the communication radius as the reachable radius. The accessibility of the coverage area of a BS is defined in the Lemma 1 and its inverse proposition shown in Lemma 2.

**Lemma 1 (Accessibility of the Coverage Area of a BS):**

For each pair of randomly deployed video surveillance devices e.g.  $d_i$  and  $d_j$  in a ring area, there always exists a UAV route  $\{d_i, a_{iL}, a_{iB}, d_j\}$  with some BSs, which guarantee the UAV can connect the above devices with energy and time constraints. Here,  $a_{iL}$  represents the BS for UAV launching and  $a_{iB}$  represents the BS for UAV landing.

*Proof:* The following issues are independent of each other: (1) deploying devices  $d_i$  and  $d_j$ , (2) initiating data of video surveillance, (3) forwarding and collecting video data. The  $d_i$  generates an independent Group Of Picture (GOP)  $X_i(k)$  and its length is  $n$ , i.e., there are  $n$  video frames in the GOP. Here,  $k \in \{1, 2, \dots, 2^{nR_i}\}$ . The  $n$  video frames of each GOP are subject to the distribution  $\prod_{k=1}^n p_i x_i(k)$ . Similarly, the  $d_j$  generates  $2^{nR_j}$  independent  $n$ -length GOP  $X_j(k)$ . The  $n$  video frames of each GOP are subject to the distribution  $\prod_{k=1}^n p_j x_j(k)$ . Here,  $P_\varepsilon^{(n)}$  represents all UAV feasible paths between devices  $d_i$  and  $d_j$ . According to the topology of BSs and the characteristics of video data transmission, each feasible path can be formalized as  $(x_i(k), x_j(k + \varepsilon), y) \in P_\varepsilon^{(n)}$ . Any small integer  $\varepsilon$  represents the difference of video data collected by two devices. The parameter  $y$  represents the set of BSs accessed by UAVs.

Define video computing events as  $M_{ij} = \{(x_i(k), x_j(k + \varepsilon), y) \in P_\varepsilon^{(n)}\}$ . The success processing probability of the video event  $P_M^{(n)} = P(\sum_{i=1}^2 M_{ij}) \leq \sum_{i=1}^2 (P(\sum_{j=1}^n M_{ij})) \leq 2^{-\frac{\varepsilon}{n}}$ . Similarly,  $P_{X_i(k)}^{(n)} \leq \frac{2^{-\frac{\varepsilon}{n}}}{|X_i(k)|}$  and  $P_{X_j(k)}^{(n)} \leq \frac{2^{-\frac{\varepsilon}{n}}}{|X_j(k)|}$ .

In summary, each pair of devices deployed randomly, e.g.  $d_i$  and  $d_j$ , always have a UAV route  $\{d_i, a_{iL}, a_{iB}, d_j\}$ . The UAV can guarantee the success of video computing event  $M_{ij}$ , i.e., to maintain the connectivity of any two devices.  $\square$

**Lemma 2 (Inverse Proposition):** For all UAV routes  $\{d_i, a_{iL}, a_{iB}, d_j\}$  with BSs that meet the energy constraint<sup>2</sup> of UAV. The devices at both ends of feasible routs must

<sup>2</sup>The energy consumption of UAV on its route does not exceed the residual energy of UAV.

be deployed in the circular rectangular annular area constrained by the BS and its coverage area.

*Proof:* Suppose there is a video event  $M_{ij}$ , satisfying the following inequalities  $P_M^{(n)} \leq 2^{-\frac{\varepsilon}{n}}$ . There is an UAV feasible path  $\{a_{i1}, a_{i2}, \dots, a_{i(q-1)}, a_{iq}\}$ . Because the monitoring events of the video surveillance devices deployed in the annular area are independent of each other and follow the same distribution. The joint distribution of any two video surveillance time slot is expressed as follows,  $p(x_i, x_j, x_i^{(n)}, x_j^{(n)}, y^n) = p(x_i^{(n)}|x_i)p(x_j^{(n)}|x_j)(\prod_{k=1}^n p(y^k|x_i, x_j))/(2^{n(R_i+R_j)})$ . When the video data difference between two endpoints of UAV path satisfies this inequality  $\|X(a_{i1}) - X(a_{iq})\| \leq \varepsilon$ , these two endpoints must be video surveillance devices at the same time.  $\square$

Some assumptions about UAV route planning based on BS are given below.

- (1) **Planar Area:** It is assumed that the video surveillance device is randomly deployed in the coverage area of the BS and the circular rectangular ring area of the accessibility plane.
- (2) **Disc Reachable Area:** The reachable area of video surveillance device and UAV is a disc, which can be defined by their position and reachable radius. The coverage area of BS means that if the video surveillance device is in this area, at least one BS can establish direct connection with it. Reachable area of BS means that UAV can launch from the current position directly to the target monitoring device for collecting and computing the video data in real time, and returning the computing results to the device. The reachable area of the video surveillance device means that the device is at least an endpoint of the UAV route containing the BSs, indicating that the UAV can connect the device with another device.
- (3) **Predictable Routes:** The bandwidth, forwarding speed and computing power of video data from BSs are known and predictable. For example, bus routes are divided into segments according to their temporal and spatial characteristics. The BS network  $N_{AP}$  consists of  $m$  BSs, denoted as  $a_{p_i}, i=1, 2, \dots, m$  and  $\sum_{i=1}^m a_{p_i} = N_{AP}$ . The flight, forwarding and computing time of UAV on  $N_{AP}$  is divided into  $u$  time slots, denoted as  $t^v, v=1, 2, \dots, u$  and  $\sum_{v=1}^u t^v = T$ . A binary  $\langle a_{p_i}, t_i^v \rangle$  is defined to represent the spatial and temporal characteristics of the BS visited by the UAV, i.e., the UAV accesses the  $i$ -th BS at the  $v$ -th time slot.
- (4) **Video Surveillance Network Of UAV:** The network consists of several UAVs, BSs and video surveillance devices.
- (5) **Video Event Processing Process:** The video event processing progress concludes the following steps: (1) the UAV launches from the initial BS, (2) the UAV accesses the target video surveillance device, and (3) the UAV returns to the initial BS and waits for the next round of video events.

- (6) *Direct Video Surveillance*: When the UAV moves to the coverage of the video surveillance device, the device uses a single-hop mode to cooperate with the UAV in video processing procedure.
- (7) *Stop Waiting Progress*: The UAV first moves to the designated location of the video surveillance device. Then, the device and the UAV establish a direct connection and collaboratively deal with the video events. Finally, the UAV leaves the current location and goes to the next device after finding the feasible path.

Then, the path planning constraints of UAV cluster based on BS network and the pre-processing scheme of its running time are given.

- (1)  $D = \{d_1, d_2, \dots, d_p\}$ . This constraint defines the set  $D$  of all video surveillance devices covered by BS network and UAV cluster.
- (2)  $N_{AP} = \{a_{p_1}, a_{p_2}, \dots, a_{p_m}\}$  and  $T = t^1, t^2, \dots, t^u$ . This constraint defines the spatial and temporal characteristics of BS network and UAV cluster.
- (3)  $AP(d_k) = \{a_{p_i} \mid \|M_{(a_{p_i}, d_k)}\| \leq \varepsilon\}$ . The constraint represents the set of all BSs that can complete video event processing for video surveillance device  $d_k$ .
- (4)  $D(a_{p_i}) = \{d_k \mid \|M_{(b_{r_i}, d_k)}\| \leq \varepsilon\}$ . This constraint represents the set of monitoring devices that successfully handle video events for UAV from the BS  $a_{p_i}$ . Here, the weights of data processing differences for video events  $\varepsilon \leq \sum_{i=1}^{|D(a_{p_i})|} P(\sum_{j=1}^n M_{ij})$ .

Based on the above constraints, the definition of video surveillance network based on UAV cluster is given below.

*Definition 1 (UAV Available Network)*: Select a subset of the BS network in the reachable area of the video surveillance device as the UAV launching or landing position of the surveillance device, which is called UAV Available Network.

UAV accessing every uncovered video surveillance device must pass through the UAV available network. Thus, it is important to find the available UAV network points for each video surveillance device. But in the intensively deployed wireless video surveillance network, the reachable areas between video surveillance devices may overlap. Therefore, the available network of two or more devices may overlap. Available network points for UAVs can be anywhere in the disk communication area of device. Since, the choice of available network points for UAVs is particularly important, which is defined as UAV route as **Definiton 2** and we can provide the feasible UAV paths constructed by multiple BSs for video events processing with UAV cluster, as shown in **Lemma 1**.

*Definition 2 (UAV Route)*: The route is a connection between the initial position of UAV and the available network points as well as video surveillance device. The line segment between the available network points of UAV on the route is simplified to a straight-line segment.

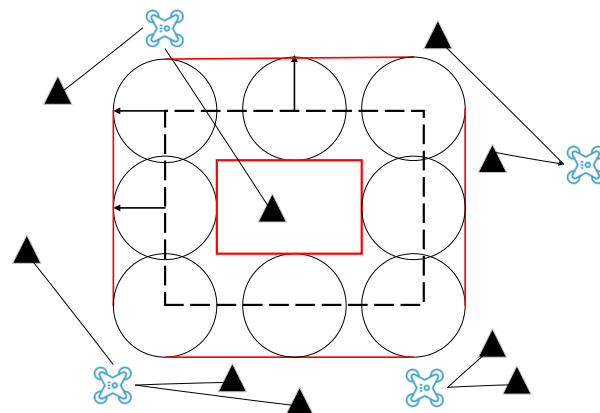


FIGURE 2. An example of Lemma 3.

*Lemma 3*: UAV can process video events and heterogeneous communication of video surveillance devices deployed on the plane through UAV paths constructed by multiple BSs.

*Proof*: Based on accessibility and its inverse proposition, the video data forwarding speed of BS and its bandwidth can be controlled completely. The feasible UAV paths can be generated. Starting from the initial position, UAV accesses all the video surveillance devices that are not directly covered by some BSs, and then returns to the initial position. Ensure that all video surveillance devices are accessed by deploying minimal UAVs. Therefore, the route planning problem of UAVs can be attributed to the bin packing problem. The problem refers to the scenarios including the video surveillance device, cooperative processing of video events, direct communication between device and UAV, and indirect communication with BS network. □

In Figure 2, the triangle represents the video surveillance device and the black arrow represents the UAV route. Graph  $G$  is composed of vertices (video surveillance devices and BSs) and their edges. By simplifying the graph  $G$ , we obtain the graph  $G' = (V', E')$ . Here,  $V' = \{UAV, d_1, d_2, \dots, d_p\}$  and  $E'$  represents the shortest path between any two vertices on  $G$ . There may be three paths between any two devices as shown in Figure 3. So, we define the UAV scheduling problem on  $G'$  as bi-objective bin packing problem following the **Definition 3**.

*Definition 3 (Bi-Objective Bin Packing Problem)*: Given some UAVs,  $p$  video surveillance devices and graph  $G'$  in a rectangular plane area, the problem is to determine the number of UAVs for determining the access sequence of all devices, i.e.,  $D = \{d_1, d_2, \dots, d_p\}$  and minimize the time cost of UAV clusters.

The problem of **Definition 3** can be formulated as follows:

$$\min \{|S|, g(S)\} \text{ s.t. } g : S \rightarrow R^+ \quad (1)$$

Here,  $S$  represents the task allocation set of the UAV cluster. Each UAV accesses each device of the bound set and completes video event processing. Here,  $S = \{s_q | (d_{p-1}, a_{p(p-1)L}, a_{p(p-1)B}, d_p)\}$ . Function  $g(S)$  denotes the

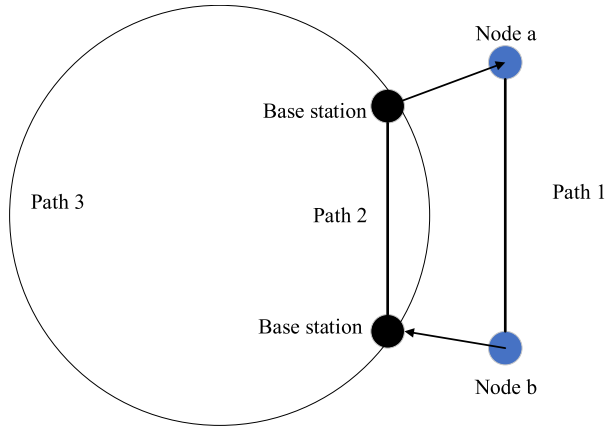


FIGURE 3. Candidate UAV paths.

time cost for all UAVs in  $S$  to complete video event processing. In  $G'$ , the edge  $e'(d_i, d_j) \in E'$  is  $\{d_i, a_{p_{iL}}, a_{p_{iB}}, d_j\}$ . The time cost on this edge is  $g(e') = t_{flying}^{d_i, a_{p_{iL}}} + t_{comm}^{a_{p_{iL}}, a_{p_{iB}}} + t_{flying}^{a_{p_{iB}}, d_j} + t_{comp}^{d_j}$ . Here,  $t_{flying}^{d_i, a_{p_{iL}}}$  represents the flying time from the current device  $d_i$  to the BS  $a_{p_{iL}}$ .  $t_{flying}^{a_{p_{iB}}, d_j}$  represents the flying time of UAV from the BS  $a_{p_{iB}}$  to the device  $d_j$ ;  $t_{comm}^{a_{p_{iL}}, a_{p_{iB}}}$  represents the communication time cost of video data between  $a_{p_{iL}}$  and  $a_{p_{iB}}$  in a BS;  $t_{comp}^{d_j}$  represents the computing time cost of UAV for handling video events at the device  $d_j$ .

#### IV. OPTIMIZATION ALGORITHM FOR HETEROGENEOUS COMMUNICATION

In order to solve the bi-objective optimization problem in **Definition 3**, we consider the following three constraints:

- (1) UAV must complete all video events assigned to it and access all video surveillance devices within a specified time.
- (2) Based on the distribution of rechargeable device, each UAV has its own task set. It is very important to plan the UAV route for ensuring the efficient access to video surveillance devices and timely completion of video event processing tasks.
- (3) The data storage and processing capability of UAV location and video surveillance device is limited.

Based on the above constrains, we give the following items of fragile packing problem: (1) items is the video surveillance devices, (2) item size is the current data storage and processing capability of device, (3) a bin is an UAV, and (4) bin capacity is the lifetime of UAV.

UAVs will access all devices before its data storage and processing capabilities are exhausted. Therefore, for these devices, UAV video event processing time is the life cycle of the device. The life cycle of a device is determined by its data storage and processing capabilities, e.g., the device will be dead when these capabilities are exhausted. The deployment and scheduling of UAV cluster is based on the principle of periodic video event processing. In a specified time,

the scheduled UAV accesses all video surveillance devices and completes video event processing tasks with the lowest energy cost.

We define  $J$  as a set of video event tasks.  $e(j)$  represents the execution time of video events on the  $j$ -th video surveillance device,  $0 < e(j) \leq 1$ . The function  $f(j)$  denotes the fragile weight of video events completed by the  $j$ -th video surveillance device. The weight can be obtained by computing the difference of data processing in video events. Based on fragile weight, we partition all devices into  $m$  subsets  $U_1, \dots, U_m$  and  $\sum_{j \in U_i} e(j) \leq 1, 1 \leq i \leq m$ . If and only if  $\beta + e(j) + t(j) \leq 1$  is satisfied, item  $j$  can be packed in a bin  $b_k$ . Here,  $\beta$  represents the current capacity of the bin  $b_k$  and  $0 < \beta \leq 1$ .  $T(j)$  represents the time cost of UAV arriving at the video surveillance device  $d_j$ . Then, UAV can complete the video event processing task from device  $d_j$  in a specified time if  $\beta + t(j) \leq e(j)$ . In addition, UAV can complete its all video event tasks before the life cycle end of the device if  $\beta + t(j) \leq \frac{1}{2}$ . So,  $e(j) \leq \frac{1}{2}$  and  $t(j) \leq \frac{1}{2}$ . The real-time requirements for UAV accessing all devices can be formulated as the following inequations,  $e(j)/\sum_{b_k} \in b_k t(i) + \sum_{b_k} b_k e(i) \geq \epsilon_j > 1$ .

Without loss of generality, we assume  $e(j) \leq f(j)$ . Otherwise, the task of the video surveillance device will never be completed. Fragile weights can be obtained by the following equation.

$$f(j) = e(j) + \frac{e(j)}{\epsilon_j} - \sum_{b_k \in b_k} t(i) \quad (2)$$

We have  $e(j)/\epsilon_j - \sum_{b_k \in b_k} t(i) \geq 0$  following  $f(j) - e(j) \geq 0$ , and  $e(j)/\epsilon_j - \sum_{b_k \in b_k} t(i) \leq \frac{1}{2}$  following  $e(j) \leq \frac{1}{2}$ , as well as  $\epsilon_j > 1$ . So,  $0 < f(j) \leq 1$ . The smaller the fragile weight  $f(j)$ , the more fragile in the item. When  $\sum_{d_j \in b_k} e(j) \leq \min\{f(1), f(2), \dots, f(|b_k|)\}$ , the above allocation scheme is feasible. Moreover, each item in  $b_k$  satisfies the inequality conditions shown in the following equation.

$$\begin{cases} \beta + t(j) \leq \frac{1}{2} \\ e(j) \leq \frac{1}{2} \\ t(j) \leq \frac{1}{2} \end{cases} \quad (3)$$

Above all, the weights sum of all items in  $b_k$  will not exceed the sum of fragile weights of the items. Since, we can solve the bin packing problem following solution  $L$  which can be obtained from the solution  $L'$ , as shown in Lemma 4.

**Lemma 4:** Bin packing solution  $L = (e(1), e(2), \dots, e(n))$  is equivalent to solution  $L' = (t(1), t(2), \dots, t(n))$ .

**Proof:** From **Lemma 2**, the problem of **Definition 3** is the same as that of Bi-objective Fragile Bin Packing (**BFBP**).  $\square$

Thus, the greedy fragile bin packing algorithm for solving the single objective sub-problem of **Definition 3** is described as Algorithm 1 and its performance bound is demonstrated in Theorem 1.

**Theorem 1:**  $w^{Algorithm1} \leq 5.4w^*$

**Algorithm 1** FBP-Greedy Algorithm

---

```

1: Sort and label all the items according to non-increasing
    $e(j)$ , e.g.  $e(1) \leq e(2) \leq \dots \leq e(n)$ ;
2:  $i \leftarrow 1, j \leftarrow 1, e \leftarrow 0, f \leftarrow f(i)$ ;
3: while  $i \leq n$  do
4:   if  $b_j \cup \{i\}$  is feasible then
5:      $b_j \leftarrow b_j \cup \{i\}$ ;
6:      $e \leftarrow e + e(i)$ ;
7:      $f \leftarrow \min\{f, f(i)\}$ ;
8:   else
9:      $j \leftarrow j + 1$ ;
10:     $b_j \leftarrow \{i\}$ ;
11:     $e \leftarrow e(i)$ ;
12:     $f \leftarrow f(i)$ ;
13:     $i + +$ ;
14:   end if
15: end while

```

---

**Algorithm 2** BFBP Algorithm

---

```

1: obtain the complete graph  $G \leftarrow (V, E)$ ;
2:  $G' \leftarrow G$ ;
3: portioning  $G'$  into  $U_1, \dots, U_m$  by using the graph coloring
   algorithm [40];
4: apply algorithm 1 to each  $U_i$ ;
5: all UAVs access the packed items according to the packing
   reverse order;

```

---

*Proof:* Let  $U_1, \dots, U_{X(G)}$  be a minimum partition of  $G$  into independent sets. We define a weighting function  $W[0, 1] \rightarrow [0, \frac{8}{5}]$  [39].

$$w(\alpha) = \begin{cases} \frac{6}{5}, & 0 \leq \alpha \leq \frac{1}{6} \\ \frac{9}{5}\alpha - \frac{1}{10}, & \frac{1}{6} < \alpha \leq \frac{1}{3} \\ \frac{6}{5}\alpha + \frac{1}{10}, & \frac{1}{3} < \alpha \leq \frac{1}{2} \\ \frac{6}{5}\alpha + \frac{4}{10}, & \frac{1}{2} < \alpha \leq 1 \end{cases} \quad (4)$$

Furthermore, let  $\bar{W}(U) = \sum_{\alpha \in U} W(e(\alpha))$ ,  $\bar{W} = \sum_{\alpha \in J} W(e(\alpha))$ ,  $\bar{T}(U) = \sum_{\alpha \in U} W(t(\alpha))$ , and  $\bar{T} = \sum_{\alpha \in J} W(t(\alpha))$ . Using a result about the weighting function [3], the number of bins generated by First Fit (FF) on a set  $U_i$  is bounded by  $\bar{W}(U_i) + \bar{T}(U_i) + 1 + 1$ . This implies that the total number of bins  $w^{\text{Algorithm 1}} \leq \sum_{i=1}^{X(G)} (\bar{W}(U_i) + \bar{T}(U_i) + 2)$ .

We assume that  $w^*(L)$  denotes the minimum number of bins in a packing for all items without the incompatibility and fragility constraint. It is clear that  $w^*(L) \leq w^*(G)$ . Therefore,  $w^{\text{Algorithm 1}} \leq \bar{W} + \bar{T} + 2X(G) \leq 1.7w^*(G) + 1.7w^*(G) + 2X(G) \leq 1.7w^*(G) + 1.7w^*(G) + 2w^*(G) = 5.4w^*(G)$ .  $\square$

After algorithm 1, we give the algorithm 2 for solving the problem of **Definition 3**. In addition, we give the Algorithm 3 to obtain the complete graph  $G$  required by Algorithm 2.

**Algorithm 3** Circles for Complete Graph

---

```

1: for  $i=1$  to  $|P|$  do
2:   while  $P \neq \emptyset$  do
3:      $P \leftarrow P/P_i$ ;
4:      $C_i^{k+1} \leftarrow \text{cycle}(P_i \text{ as a center and } kR \text{ as radius})$ ;
5:     if  $\exists$  points  $\in P$  and covered by  $C_i^1$  then
6:       connect  $P_i$  with the above points;
7:     end if
8:      $P \leftarrow P/$  the above points
9:      $R_{\text{ing}} \leftarrow$  the ring between  $C_i^{k+1}$  and  $C_i^k$ ;
10:     $VDC \leftarrow$  the video devices covered by  $R_{\text{ing}}$ ;
11:    for  $j = 0$  to  $|P/P_i|$  do
12:      connect  $P_i$  and  $P_j$  with the directed line  $P_iP_j$ ;
13:      for  $u = 1$  to  $\lceil \frac{|P_iP_j|}{R} \rceil$  do
14:         $OPT_j^k \leftarrow$  intersections of  $P_iP_j$  with  $C_i^k$ ;
15:         $VD_{ok}^{u,j} \leftarrow$  algorithm 4 ( $OPT_j^k, VD_{ok}^{u-1,j}$ );
16:      end for
17:    end for
18:    if  $(VD_{ok}^{u,j}, P_j) \geq R$  then
19:       $VD_{ok}^{u+1,j} \leftarrow$  algorithm 4 ( $P_j, VD_{ok}^{u,j}$ );
20:    end if
21:  end while
22: end for

```

---

**Algorithm 4** Refine the Candidates

---

```

1: for  $m = 1$  to  $|VDC|$  do
2:   compute the distance between  $VDC_m$  and  $OPT_{ok}^k$ ;
3: end for
4: for  $n = 1$  to  $|VDC|$  do
5:   resort  $BSC$  with ascending order of distance;
6: end for
7: for  $q = 1$  to  $|VDC|$  do
8:   if  $(VDC_q, VD_{ok}^{u-1,j}) \leq R$  then
9:      $VD_{ok}^{u,j} \leftarrow VD_q$ ;
10:    return  $VD_{ok}^{u,j}$ ;
11:   end if
12: end for

```

---

The notations in the above algorithms are demonstrated by Table 1.

**V. EXPERIMENTAL ANALYSIS AND VERIFICATION**

In order to verify the performance of the proposed algorithm in real-time and reliability of video surveillance network, we designed a series of simulation experiments which are implemented by using MATLAB and C, the video data in Table 2 are processed according to the experimental environment in Table 3.

We compare the video surveillance network without UAV (UAV-NULL), distance greedy UAV scheduling strategy (UAV-DG) and the proposed algorithm (UAV-CO) in terms of system life cycle, video decodable frame rate, UAV flight

TABLE 1. Notations.

Notation	Definition
$X_j(k)$	GOP
$P_\varepsilon^{(n)}$	all UAV feasible paths between devices $d_i$ and $d_j$
$D$	Video surveillance device set
$N_{AP}$	Wireless base stations set
$t_{fly}^{d_i, a_{p_{iL}}}$	the flying time from $d_i$ to $a_{p_{iL}}$ .
$t_{fly}^{a_{p_{iB}}, d_j}$	the flying time from $a_{p_{iB}}$ to device $d_j$ .
$t_{comm}^{a_{p_{iL}}, a_{p_{iB}}}$	the communication time between $a_{p_{iL}}$ and $a_{p_{iB}}$ .
$t_{comp}^{d_j}$	the computing time of UAV handling video events at $d_j$
$d_i$	$i$ -th video surveillance device
$e(j)$	the execution time of $j$ -th device to complete video events
$\beta$	the current capacity of the bin $b_k$
$U_1, \dots, U_{X(G)}$	a minimum partition of $G$ into independent sets
$f(j)$	the fragile weight of $j$ -th item
$b_j$	the $j$ -th bin
$w^*(L)$	the weight sum of optimal UAV path $L$
$C_i^{k+1}$	the cycle of $i$ -th UAV at $(k+1)$ -th time slot
$OPT_{ok}^k$	the optimal device at $k$ -th iteration
$R$	visible distance of UAV
$VDC_q$	the candidate video devices at $q$ time slot
$VD_{ok}^{u,j}$	the $j$ -th optimal video device of the $u$ -th UAV
$a_{iL}$	the base station for UAV launching
$a_{iB}$	the base station for UAV landing.

TABLE 2. Settings of environment.

Parameters	Value
$N_{AP}$	[1, 20]
Number of UAVs	[1, 10]
Size of monitoring area	900m*1200m
Maximum ascent speed: motion mode	5 m/s
Maximum descent rate	3 m/s
Maximum horizontal flight speed	45 km/h
Maximum takeoff altitude	2000 m
Longest communication range	13 km

TABLE 3. Settings of video.

Parameters	Value
Video coding scheme	AVC (h, 264) Level 2
Video Resolution	640X360 (nHD)
Video Bit Rate	512 kbps-1 Mbps
Video frame rate	30 FPS
Audio Coding	AAC-LC
Audio Bit Rate	96 kbps-192 kbps
Number of video frames	13678 frames
Time of video	65.45 minutes
Number of frames in a GOP	12 frames

time ratio, throughput and delay. The detailed description of the above comparison algorithms are given as follows:

- (1) **UAV-NULL**. In this algorithm, video surveillance devices are divided into two categories: some covered by **BS** network and others uncovered. At this time, the collection, forwarding and processing of video data are completed by the cooperation of **BS** and monitoring device.
- (2) **UAV-DG**. In this algorithm, UAV prefers to serve the nearest video surveillance device. At this time, there will be the worst case: the video surveillance event of

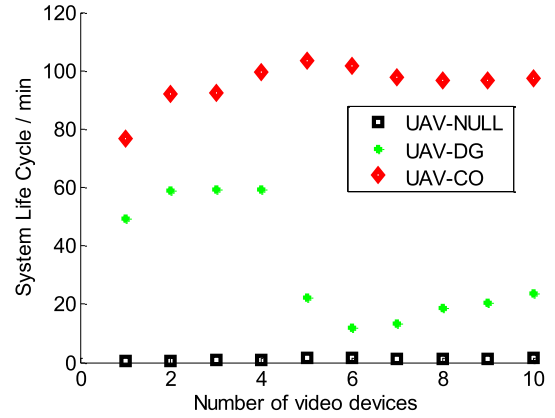


FIGURE 4. System life cycle vs. Number of video devices.

the nearest monitoring device is the monitoring state, e.g., no video data. Devices in urgent state, i.e., they have urgent UAV data service requirements, cannot be responded because of their long distance.

- (3) **UAV-CO**. This algorithm is based on Algorithms 1, 2, 3 and 4.

The comparative performance metrics mentioned above are as follows:

- (1) *System life cycle*. The time between the first video frame sent by the video surveillance device and the last video frame received by the **BS**.
- (2) *Video decodable frame rate*. The ration of the correct decoded video frames received by **BSs** to the total video frames received.
- (3) *Flying time ratio*. The ratio of the flying time of UAV to the system time.
- (4) *Throughput*. The ratio of decodable video data received by **BSs** to the total video data.
- (5) *Delay*. The average time cost between the **BSs** to decode the video frame correctly.

Figure 4 and 5 show the lifecycle of video surveillance network system of three algorithms with different number of devices and **BSs**. The results show that the system cycle of **UAV-NULL** is the shortest, and this conclusion is obvious. The lifetime of **UAV-CO** is prolonged by about 50% compared with that of **UAV-DG**. This is because **UAV-CO** can find a feasible UAV route between every pair of devices. The UAV can ensure the success of the video computing event  $M_{ij}$ , i.e., to maintain the connectivity of any two devices. This connectivity enables UAVs to provide data collection, forwarding and computing services, as well as effectively prolong the life cycle of the system.

Figure 6 and 7 show the video decodable frame rates with different number of devices and **BSs**. The decodable frame rate of **UAV-NULL** is not only very jittery, but also very low. There always exist some devices which cannot be covered by **BSs** and submit the complete video frames. According to Lemma 1 and 2, the proposed algorithm **UAV-CO** can respond to events in time and obtain video surveillance data

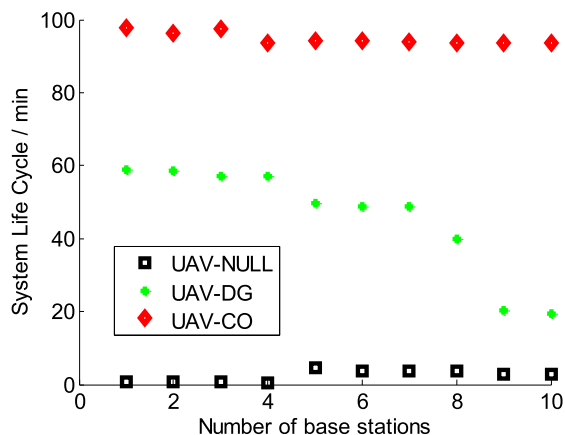


FIGURE 5. System life cycle vs. Number of base stations.

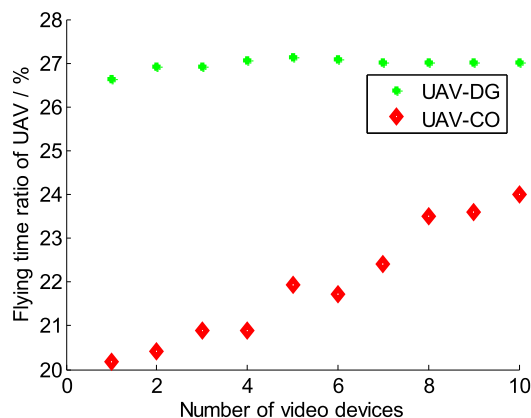


FIGURE 8. Flying time ratio of UAV vs. Number of video devices.

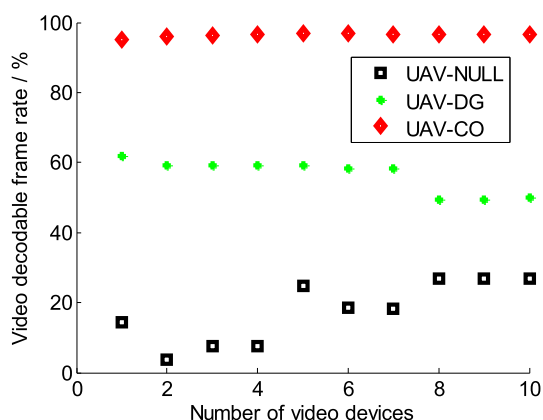


FIGURE 6. Video decodable frame rate vs. Number of video devices.

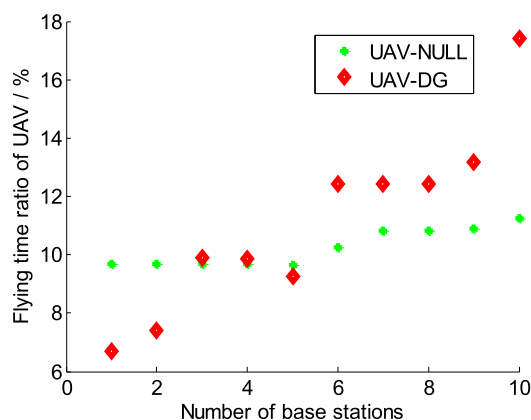


FIGURE 9. Flying time ratio of UAV vs. Number of base stations.

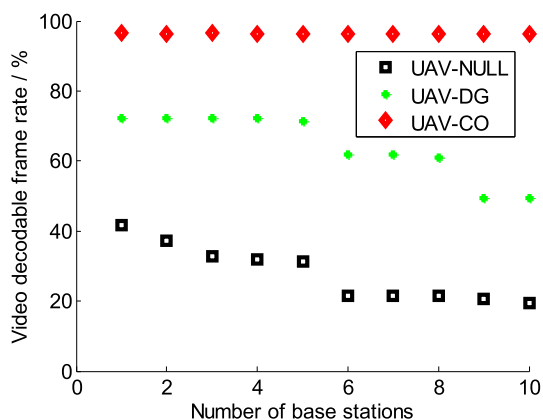


FIGURE 7. Video decodable frame rate vs. Number of base stations.

with high probability. And, it can detect the difference of video data between two positions of UAV path in time. According to the problem described in equation (1), it can fully maximize the video surveillance events per unit time, collect and decode video frames. So, the decodable frame rate of the proposed algorithm is always high. We also found that the decodable frame rate of the proposed algorithm is about 20% higher than that of UAV-DG.

Figure 8 and 9 show the flight time ratio of UAV between two algorithms in different number of devices and BSs. It is found that UAV-NULL not only has longer flight time than the proposed algorithm, but also has more flight time in large-scale video surveillance network. Although we find that the flight time of UAV based on the proposed algorithm is on the rise, the increase is relatively low. This is because the execution time of Algorithm 1 is complex, which makes UAV hover in the air for a certain time. But it will not exceed the energy limitation of UAV. In addition, the simplification of  $G$  is helpful to improve the efficiency and accuracy of UAV route decision-making. We found that the UAV flight time of the proposed algorithm is about 10% less than that of UAV-DG.

Figure 10 and 11 show the throughput of the three algorithms for video communication. From Figure 11, the throughput of UAV-NULL is very close to that of UAV-DG when the number of BS equals to 8. This is a very interesting result. Because there are some uncovered devices in UAV-NULL, the throughput is always at a low level. However, the UAV-DG focuses on distance greed. When multiple UAVs serve the same video surveillance device simultaneously or sequentially, the throughput is equivalent to UAV-NULL. In addition, we find that the throughput of the proposed algorithm is always above 95%. This is because



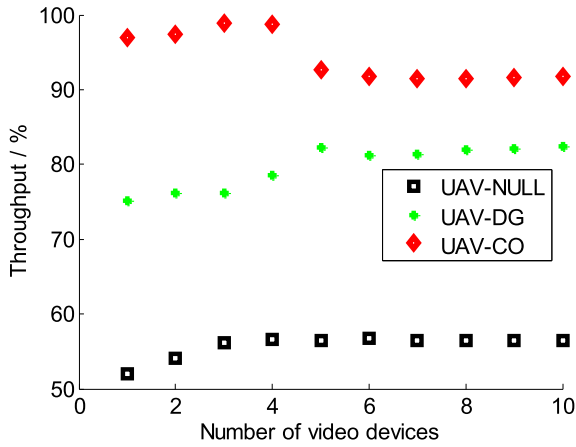


FIGURE 10. Throughput vs. Number of video devices.

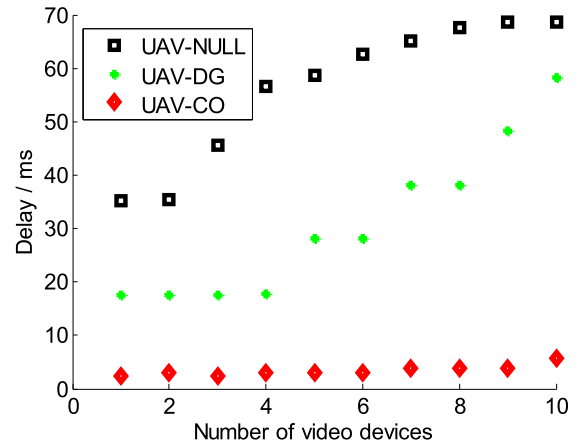


FIGURE 12. Delay vs. Number of video devices.

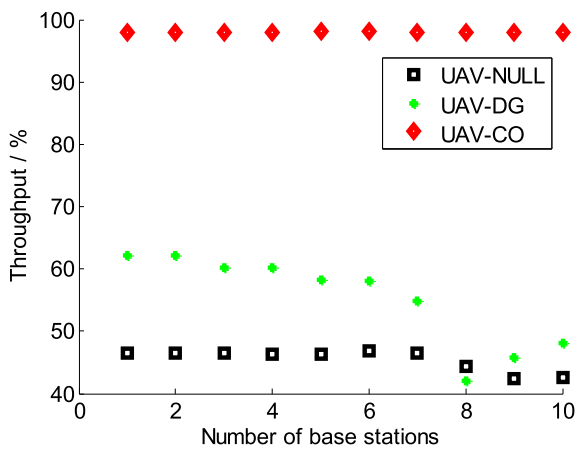


FIGURE 11. Throughput vs. Number of base stations.

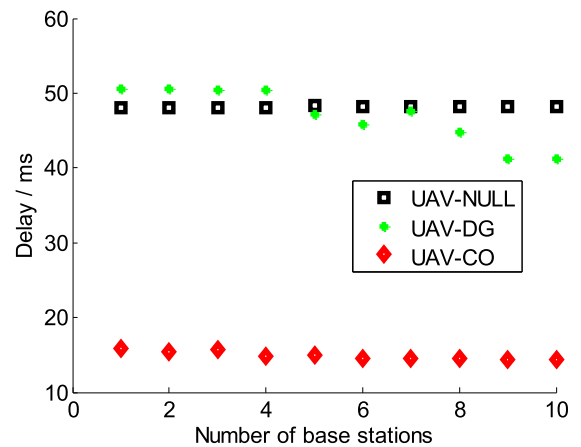


FIGURE 13. Delay vs. Number of base stations.

the implementation of Algorithm 3 makes the mapping efficiency between UAV and video surveillance device high, and improves the throughput of video communication. We found that the throughput of the proposed algorithm is at least 15% higher than that of UAV-DG and 35% higher than that of UAV-NULL.

Figure 12 and 13 show the average delay of video communication under different number of devices and BSs. It is found that the delay of UAV-NULL is very close to the delay of UAV-DG. This is also a very interesting result. Because there are some BSs in UAV-NULL scheme. There are some video frames waiting for forwarding in the buffer queues of these BSs, which leads to the increase of the forwarding delay of some video frames. Similarly, UAV-DG scheme takes distance greed as its core, which can make some UAVs play the role of cooperative BSs with large buffer queues. When multiple UAVs serve the same video surveillance device simultaneously or sequentially, the communication between the BS and the UAV is congested for a long time, which leads to the increase of transmission delay. The delay of the proposed algorithm is reduced by at least 150% compared

with UAV-DG and increased by at least 45% compared with UAV-NULL.

## VI. CONCLUSION

In this paper, we designed an efficient and reliable UAV cluster-based video surveillance system optimization algorithm in heterogeneous communication of smart cities. At first, we show the video surveillance network based on UAV cluster by using the BSs network and accessibility of UAV cluster. Then, we defined the bi-objective bin packing problem for resolving the optimization of UAV cluster. And, the algorithm 1 was given by using the greedy fragile bin packing algorithm. It has a constant approximation ratio following the Theorem 1. Additionally, algorithm 2, 3 and 4 were given for addressing the BFBP problem, obtaining the circles for complete graph, and refining the candidates of UAV route, respectively. Finally, our simulation results demonstrate that our proposed solution can be efficiently and feasibly applied to video surveillance application in smart city. Specially, the proposed algorithms can achieve about 50% system life cycle extension compared to that of UAV-DG, 20% video decodable ratio improvement compared to

that of **UAV-DG**. In addition, the UAV flying time ratio of the proposed algorithm is 10% less than one of **UAV-DG**. Throughput is at least 15% higher than that of **UAV-DG** and 35% higher than that of **UAV-NULL**. Delay is reduced by at least 150% compared with **UAV-DG**.

## REFERENCES

- [1] X. Wang, "Intelligent multi-camera video surveillance: A review," *Pattern Recognit. Lett.*, vol. 34, no. 1, pp. 3–19, Jan. 2013.
- [2] E. Mueggler, H. Rebecq, T. Delbruck, D. Scaramuzza, and G. Gallego, "The event-camera dataset and simulator: Event-based data for pose estimation, visual odometry, and SLAM," *Int. J. Robot. Res.*, vol. 36, no. 2, pp. 142–149, 2017.
- [3] Z. Zhi-Rong, S. Peng-Shuai, and P. Tao, "Application of laser absorption spectroscopy for identification gases in industrial production processes and early safety warning," *Opt. Precis. Eng.*, vol. 26, no. 8, pp. 1925–1937, 2018.
- [4] H. Prihadi and M. Djamil, "The reliability of wireless sensor network on pipeline monitoring system," *J. Math. Fundam. Sci.*, vol. 49, no. 1, pp. 51–56, 2017.
- [5] A. K. Jägerbrand and H. Antonson, "Driving behaviour responses to a moose encounter, automatic speed camera, wildlife warning sign and radio message determined in a factorial simulator study," *Accident Anal. Prevention*, vol. 86, pp. 229–238, Jan. 2016.
- [6] M. Pouryazdan, B. Kantarci, T. Soyata, and H. Song, "Anchor-assisted and vote-based trustworthiness assurance in smart city crowdsensing," *IEEE Access*, vol. 4, pp. 529–541, 2017.
- [7] Y. Wang, X. X. Zhu, B. Zeisl, and M. Pollefeys, "Fusing meter-resolution 4-D InSAR point clouds and optical images for semantic urban infrastructure monitoring," *IEEE Trans. Geosci. Remote Sens.*, vol. 55, no. 1, pp. 14–26, Jan. 2017.
- [8] H. Mollenhauer, M. Kasner, P. Haase, J. Peterseil, C. Wohner, M. Frenzel, M. Mirtl, R. Schima, J. Bumberger, and S. Zacharias, "Long-term environmental monitoring infrastructures in Europe: Observations, measurements, scales, and socio-ecological representativeness," *Sci. Total Environ.*, vol. 624, pp. 968–978, May 2018.
- [9] Z. Cai, L. Deng, X. Yao, D. Cox, H. Wang, and D. Li, "A FCM cluster: Cloud networking model for intelligent transportation in the city of Macau," *Cluster Comput.*, vol. 22, pp. 1219–1228, Oct. 2017.
- [10] R. I. Meneguet, A. Boukerche, and A. H. M. Pimenta, "AVARAC: An availability-based resource allocation scheme for vehicular cloud," *IEEE Trans. Intell. Transp. Syst.*, vol. 20, no. 10, pp. 3688–3699, Oct. 2018.
- [11] Y. Luo, S.-C.-S. Cheung, R. Lazerretti, T. Pignata, and M. Barni, "Anonymous subject identification and privacy information management in video surveillance," *Int. J. Inf. Secur.*, vol. 17, no. 3, pp. 261–278, Jun. 2018.
- [12] V. H. Dale and K. L. Kline, "Interactive posters: A valuable means of enhancing communication and learning about productive paths toward sustainable bioenergy," *Biofuels, Bioproducts Biorefining*, vol. 11, no. 2, pp. 243–246, Mar. 2017.
- [13] M. Monti and S. Rasmussen, "RAIN: A bio-inspired communication and data storage infrastructure," *Artif. Life*, vol. 23, no. 4, pp. 552–557, Nov. 2017.
- [14] D. Mishra, G. C. Alexandropoulos, and S. De, "Energy sustainable IoT with individual QoS constraints through MISO SWIPT multicasting," *IEEE Internet Things J.*, vol. 5, no. 4, pp. 2856–2867, Aug. 2018.
- [15] E. Pashajavid, F. Shahnia, and A. Ghosh, "Provisional internal and external power exchange to support remote sustainable microgrids in the course of power deficiency," *IET Gener., Transmiss. Distrib.*, vol. 11, no. 1, pp. 246–260, Jan. 2017.
- [16] M. Du, K. Wang, X. Liu, S. Guo, and Y. Zhang, "A differential privacy-based query model for sustainable fog data centers," *IEEE Trans. Sustain. Comput.*, vol. 4, no. 2, pp. 145–155, Apr. 2019.
- [17] A. Gomez, M. Magno, M. F. Lagadec, and L. Benini, "Precise, energy-efficient data acquisition architecture for monitoring radioactivity using self-sustainable wireless sensor nodes," *IEEE Sensors J.*, vol. 18, no. 1, pp. 459–469, Jan. 2018.
- [18] W. Sun and J. Liu, "Congestion-aware communication paradigm for sustainable dense mobile crowdsensing," *IEEE Commun. Mag.*, vol. 55, no. 3, pp. 62–67, Mar. 2017.
- [19] A. Bilzhause, B. Belgacem, M. Mostafa, and T. Graupl, "Datalink security in the L-band digital aeronautical communications system (LDACS) for air traffic management," *IEEE Aerosp. Electron. Syst. Mag.*, vol. 32, no. 11, pp. 22–33, Nov. 2017.
- [20] S. Shreejith, L. K. Mathew, V. A. Prasad, and S. A. Fahmy, "Efficient spectrum sensing for aeronautical LDACS using low-power correlators," *IEEE Trans. Very Large Scale Integr. (VLSI) Syst.*, vol. 26, no. 6, pp. 1183–1191, Jun. 2018.
- [21] H. Menouar, I. Guvenc, K. Akkaya, A. S. Uluogac, A. Kadri, and A. Tuncer, "UAV-enabled intelligent transportation systems for the smart city: Applications and challenges," *IEEE Commun. Mag.*, vol. 55, no. 3, pp. 22–28, Mar. 2017.
- [22] R. Ke, Z. Li, J. Tang, Z. Pan, and Y. Wang, "Real-time traffic flow parameter estimation from UAV video based on ensemble classifier and optical flow," *IEEE Trans. Intell. Transp. Syst.*, vol. 20, no. 1, pp. 54–64, Jan. 2019.
- [23] P. Derian and R. Almar, "Wavelet-based optical flow estimation of instant surface currents from shore-based and UAV videos," *IEEE Trans. Geosci. Remote Sens.*, vol. 55, no. 10, pp. 5790–5797, Oct. 2017.
- [24] S. Liu, S. Wang, W. Shi, H. Liu, Z. Li, and T. Mao, "Vehicle tracking by detection in UAV aerial video," *Sci. China Inf. Sci.*, vol. 62, no. 2, Feb. 2019. Art. no. 24101
- [25] B. Kalantar, S. B. Mansor, A. Abdul Halin, H. Z. M. Shafri, and M. Zand, "Multiple moving object detection from UAV videos using trajectories of matched regional adjacency graphs," *IEEE Trans. Geosci. Remote Sens.*, vol. 55, no. 9, pp. 5198–5213, Sep. 2017.
- [26] Z. Sun, Q. Zhang, Y. A. Tan, and Y. Li, "DPPDL: A dynamic partial-parallel data layout for green video surveillance storage," *IEEE Trans. Circuits Syst. Video Technol.*, vol. 28, no. 1, pp. 193–205, Aug. 2018.
- [27] T. Sentenac, Y. Le Maout, G. Boucourt, and J. J. Orteu, "Evaluation of a charge-coupled-device-based video sensor for aircraft cargo surveillance," *Opt. Eng.*, vol. 41, no. 4, pp. 796–810, 2018.
- [28] Z. Shao, J. Cai, and Z. Wang, "Smart monitoring cameras driven intelligent processing to big surveillance video data," *IEEE Trans. Big Data*, vol. 4, no. 1, pp. 105–116, Mar. 2018.
- [29] W. Huang, H. Ding, and G. Chen, "A novel deep multi-channel residual networks-based metric learning method for moving human localization in video surveillance," *Signal Process.*, vol. 142, pp. 104–113, Jan. 2018.
- [30] D. Samaiya and K. K. Gupta, "Intelligent video surveillance for real time energy savings in smart buildings using HEVC compressed domain features," *Multimedia Tools Appl.*, vol. 77, no. 21, pp. 29059–29076, Nov. 2018.
- [31] R. Du, P. Santi, M. Xiao, A. V. Vasilakos, and C. Fischione, "The sensible city: A survey on the deployment and management for smart city monitoring," *IEEE Commun. Surveys Tuts.*, vol. 21, no. 2, pp. 1533–1560, 2nd Quart., 2019.
- [32] R. Zhang, S. Newman, M. Ortolani, and S. Silvestri, "A network tomography approach for traffic monitoring in smart cities," *IEEE Trans. Intell. Transp. Syst.*, vol. 19, no. 7, pp. 2268–2278, Jul. 2018.
- [33] J. Kharel, H. T. Reda, and S. Y. Shin, "Fog computing-based smart health monitoring system deploying LoRa wireless communication," *IETE Tech. Rev.*, vol. 36, no. 1, pp. 69–82, Jan. 2018.
- [34] A. H. Meghdadi and P. Irani, "Interactive exploration of surveillance video through action shot summarization and trajectory visualization," *IEEE Trans. Vis. Comput. Graphics*, vol. 19, no. 12, pp. 2119–2128, Dec. 2013.
- [35] Z. Xue, J. Wang, Q. Shi, G. Ding, and Q. Wu, "Time-frequency scheduling and power optimization for reliable multiple UAV communications," *IEEE Access*, vol. 6, pp. 3992–4005, 2018.
- [36] Y. Khosiawan, Y. Park, I. Moon, J. M. Nilakantan, and I. Nielsen, "Task scheduling system for UAV operations in indoor environment," *Neural Comput. Appl.*, vol. 31, no. 9, pp. 5431–5459, Sep. 2019.
- [37] Y. Cai, F. Cui, Q. Shi, M. Zhao, and G. Y. Li, "Dual-UAV-enabled secure communications: Joint trajectory design and user scheduling," *IEEE J. Sel. Areas Commun.*, vol. 36, no. 9, pp. 1972–1985, Sep. 2018.
- [38] C. Yin, Z. Xiao, X. Cao, X. Xi, P. Yang, and D. Wu, "Offline and online search: UAV multiobjective path planning under dynamic urban environment," *IEEE Internet Things J.*, vol. 5, no. 2, pp. 546–558, Apr. 2018.
- [39] M. R. Garey, R. L. Graham, D. S. Johnson, and A. C.-C. Yao, "Resource constrained scheduling as generalized bin packing," *J. Combinat. Theory A*, vol. 21, no. 3, pp. 257–298, Nov. 1976.
- [40] H. Lu, M. Halappanavar, D. Chavarria-Miranda, A. H. Gebremedhin, A. Panyala, and A. Kalyanaraman, "Algorithms for balanced graph colorings with applications in parallel computing," *IEEE Trans. Parallel Distrib. Syst.*, vol. 28, no. 5, pp. 1240–1256, May 2017.



**YONG JIN** received the M.S. degree in computer application technology from Nanjing Tech University, in 2009. He is currently an Associate Professor with the School of Computer Science and Engineering, Changshu Institute of Technology. His current research interests include edge/fog computing, wireless charging systems, the Industrial Internet of Things, and so on.



**WEIYONG YANG** is currently a Senior Engineer. His current research interests include the information safety and so on.

...



**ZHENJIANG QIAN** received the Ph.D. degree from the Computer Science and Technology Department, Nanjing University, in September 2013. In 2013, postdoctoral and collaborative research was conducted at King's College, University of London. He is currently an Associate Professor with the School of Computer Science and Engineering, Changshu Institute of Technology. He is mainly engaged in scientific research on the formalization of operating systems.